

Wheel rolling on deformable ground with slippage

Alexey Mamaev^{1*}, Tatiana Balabina², and Maria Karelina²

¹Moscow Polytechnic University (Mospolytech), BolshayaSemyonovskaya str., 38, Moscow 107023, Russia

²Moscow Automobile and Road Construction State Technical University (MADI), 64, Leningradsky prospect, Moscow 125319, Russia

Abstract. Wheeled vehicles can move not only on a solid supporting surface, but also on deformable surfaces (snow, ground, sand, etc.). When a pneumatic wheel with a high internal air pressure rolls over deformable soil, the nature of the wheels' interaction with the ground is such that the wheel can be considered rigid, since its normal deformation is small. This greatly simplifies the calculations associated with the analysis of the wheeled vehicles' operation, taking into account the transforming properties of the wheel mover, in particular, the determination of the kinematic and power parameters of the wheel. In this paper, using the method of motion reversal, the picture of physical phenomena in the contact of the wheel with the ground is considered, which made it possible to obtain relatively simple expressions for calculating the circumferential traction force and the coefficient of tangential elasticity of the "wheel - deformable ground" pair.

1 Introduction

The movement and performance of wheeled vehicles is largely determined by the interaction of the wheels with the supporting surface. Therefore, the study of the mechanics of rolling wheels is of both scientific and practical interest. A large number of studies, such as [Balabina, T.A. et al (2019), Balabina, T.A. et al (2020), Balakina, E.V. (2019), Balakina, E.V. et al (2021), Bakker ,et al (1973), Cho, J. et al (2015), Clark, S.K. (1983), Emami, A., et al.(2017), Ginzburg, G. et al (2017), Gim, G. (1990), Jimenez, E., Sandu C. (2020), Karelina, M.Y. et al (2019), Karelina, M.Y. et al (2020), M.Yu.Karelina, T.A.Balabina et al (2020), M.Yu.Karelina, T.A.Balabina et al (2021), Khaleghian, S., Ghasemalizadeh, O., and Taheri, S. (2016), Kubba, A.I. et al (2018), Li, J., Zhang, Y., Yi, J. (2012), Liang, W., Medanic, J., Ruhl, R. (2008), Mamaev, A.N., Balabina, T.A., Odinokova, I.V., Gaevskiy, V.V. (2019), Marco, Viehweger et al (2020), Ozaki, S., Kondo, W. (2016), Pacejka, H.B. (2012), Viehweger, M., et al. (2020), Wong ,J. (1982), Zadvornov, V.N. et al. (2020)], is devoted to the rolling of wheels on a rigid supporting surface. However, there are a variety of wheeled vehicles designed to work on deformable soils. This necessitates consideration of the features of the interaction of elastic wheels with the ground, including the determination of the forces and moments acting on the wheels [Becker, M.G. (1973), Fujiwara, D.,

* Corresponding author: mamist-man@rambler.ru

Tsujikawa, N., Oshima, T. et al, (2021), Kurjenluoma, J., Alakukku, L., Ahokas, J., (2009), L. ten, Damme, P., Schjonning, L.J., Munkholm et al. ,(2021), Mamaev, A., Balabina, T., Karelina, M.,(2020), Papamichael, S., Vrettos, C., (2021), Pryadkin, V, Artemov, A, Kolyadin, P. (2021), Viehweger, M., et al., (2020), Wong, J. (1982)].

A number of studies in their models take into account the viscoelastic properties of the soil-wheel system, but the dependences used in this case lead to complex expressions that make their practical use difficult, and, moreover, require more experimental data.

A significant amount is devoted to determining the radii of rolling and slipping of wheels on deformable soil, since these quantities are usually included in equations that make it possible to determine the power parameters of wheel propellers and the traction and dynamic performance of a wheeled vehicle as a whole. In this case, there is a great variety of solutions due to various initial models of the interaction of wheels with the ground. The vast majority of these solutions are cumbersome and difficult to perceive.

When a pneumatic wheel with a high internal air pressure rolls over deformable soil, the nature of the interaction of the wheels with the ground is such that the wheel can be considered rigid, since its normal deformation is small. This greatly simplifies the calculations associated with the analysis of the operation of wheeled vehicles, which was used, in particular, by Balabina et al. [Balabina, T.A., Karelina, M.Yu., Mamaev, A.N., 2021], Pirkovsky Yu.V., Babkov B.F. [Babkov, V.F., 1955, Babkov, V.F. et al., 1959], Govorushchenko N.Ya. [Govorushchenko N.Ya., 1971], Bakker M.G. [Bakker M.G., et al. (1973)], Mamaev A.N. et al. [Mamaev, A., Balabina, T., Karelina, M., 2020], Wong, J. [Wong, J. 1982], and others.

2 Materials and methods

Let us consider rolling of a wheel on deformable ground, which is rigid in the radial direction and has circumferential compliance (which corresponds to the wheel model “elastic band on a rigid rim”).

In this case, we will make an assumption about the elastic properties of the soil, i.e., we will assume that, up to a certain limit, there is a linear relationship between the tangential (with respect to the wheel surface) soil displacements and the limiting tangential forces in the contact zone.

For the convenience of solving the problem, we use an inverted mechanism (i.e., the wheel axis is stationary, and the base (ground) moves at a speed of V in the direction opposite to the actual direction of the wheel movement (Fig. 1), similar to how it was used in [Balabina, T.A. et al (2019), Balabina, T.A. et al (2020), Karelina, M.Y. et al (2019), Mamaev, A.N., et al (2019)].

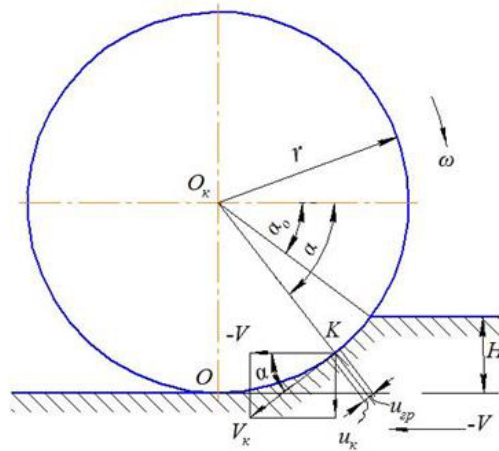


Fig. 1. Determination of tangential displacements of wheel and ground surface points in the contact zone.

Let us consider the motion of point K, which simultaneously belongs to both the wheel and the ground in the contact zone in the adhesion area.

During the time corresponding to the rotation of the wheel from the moment point K enters into contact with the ground to its position determined by the angle α , the tangential displacement of the ground point will be U_{GR} , and the tangential displacement of the wheel point (relative to the ray on which this point was located before contact) - U_K .

The speed of point K of the wheel surface in the inverted mechanism in the absence of tangential displacements is equal to the value $V_{K_{a.t.d.}} = -\omega r$.

The actual speed of the considered point in the presence of a tangential displacement can be presented in the form:

$$V_K = V_{K_{a.t.d.}} + \frac{dU_K}{dt}, \quad (1)$$

where dU_K - increment of the tangential displacement of the wheel point during the time $dt=dx/V$ (it is negative for the driving wheel, it is positive for the driven and brake wheels), dx is the elementary movement (increment) of the base (ground) in the horizontal direction in the inverted mechanism.

Similarly, one can represent the same speed of the same point by referring it to the base:

$$V_{GR} = V_{GR_{a.t.d.}} + \frac{dU_{GR}}{dt} \quad (2)$$

Here dU_{GR} - increment of the tangential displacement of a point on the ground surface over the same time interval; $V_{GR_{a.t.d.}} = -V / \sin \alpha$ - the speed of a given base point in an inverted mechanism, i.e., in the absence of tangential displacements.

Since expressions (1) and (2) represent the same speed of point K, then, by equating their right parts, after transformations we obtain:

$$d(U_{GR} - U_K) = (V_{K_{a.t.d.}} - V_{GR_{a.t.d.}}) dt = \left(\frac{V}{\sin \alpha} - \omega r \right) \frac{dx}{V} = \left(\frac{1}{\sin \alpha} - \frac{r}{r_k} \right) dx \quad (3)$$

Taking into account that $\sin \alpha = \sqrt{r^2 - x^2} / r = \sqrt{1 - x^2 / r^2}$, the expression $1/\sin \alpha$ after expanding it into a power series and discarding the values of the second and more orders of smallness, can be represented as:

$$1/\sin \alpha \approx 1 + x^2 / 2r^2$$

Substituting the last expression (3), we obtain:

$$dU = d(U_{GR} - U_K) = \left(1 + \frac{x^2}{2r^2} - \frac{r}{r_k} \right) dx \quad (4)$$

As a result, for the position of point K, determined by the x coordinate, in the adhesion section

$$U = \int_0^x dU = \left(1 - \frac{r}{r_k} \right) x + \frac{x^3}{6r^2} + c \quad (4')$$

Taking into account the boundary conditions (when $x=a$ $U=0$), after finding the constant c, we finally have:

$$U = \left(\frac{r}{r_k} - 1 \right) (a - x) - \frac{a^3 - x^3}{6r^2} \quad (4)$$

The specific tangential forces (tangential stresses) acting at a given point on the wheel and on the ground are equal in magnitude but opposite in direction: $q_t = q_{t_k} = -q_{t_{GR}}$. Under the assumption that the specific tangential forces are proportional to tangential displacements, the last equality can be represented as:

$$\lambda_k U_K = -\lambda_{GR} U_{GR}, \quad (5)$$

where λ_k and λ_{GR} - coefficients of tangential stiffness of the wheel and soil.

Expressing the U_{GR} value from equality (5) and substituting it into formula (4), after transformations, we obtain an expression for the tangential displacements of points on the wheel surface, and then the ground:

$$U_K = \frac{\lambda_{GR}}{\lambda_K + \lambda_{GR}} U \quad U_{GR} = \frac{-\lambda_K}{\lambda_K + \lambda_{GR}} U \quad (6)$$

Thus, the specific tangential forces acting at the considered point of the adhesion section will be represented by the dependencies:

$$q_{t_k} = \frac{\lambda_k \lambda_{GR}}{\lambda_K + \lambda_{GR}} U \quad q_{t_{GR}} = \frac{-\lambda_k \lambda_{GR}}{\lambda_K + \lambda_{GR}} U$$

or

$$q_t = q_{t_k} = -q_{t_{GR}} = \lambda_{np} U, \quad (7)$$

where

$$\lambda_{np} = \frac{\lambda_K \lambda_{GR}}{\lambda_K + \lambda_{GR}} \quad (8)$$

- reduced coefficient of tangential stiffness of the wheel-ground pair. Expressions (4) and (7) determine, respectively, tangential displacements and specific tangential forces, which are determined both by the realization of the circumferential force in the contact and by the geometry of the contact zone.

With the adopted wheel rolling model, even when significant, close to the limiting forces in terms of adhesion, the coordinate of the boundary of the adhesion and sliding sections is $x_B=0$.

The tangential stresses distributed along the arc of a circle in the contact zone create a moment relative to the center of the wheel:

$$M_t = \int_{\alpha_0}^{\pi/2} 2bq_t r r d\alpha = 2br^2 \lambda_{np} \int_{\alpha_0}^{\pi/2} U d\alpha \quad (9)$$

Let's use this expression to find the rolling radius r_{k_0} , at which $M_t=0$. Substituting equation (4) into (9) and equating the expression obtained after transformations to zero, we obtain:

$$r_{k_0} = r / (1 + a^2 / 4r^2) \approx r - a^2 / 4r = r - H / 2 \quad (10)$$

Taking into account this formula, from (4) we obtain a dependence that determines the law of change of tangential displacements in the contact zone, at which the torque on the wheel, due to the presence of tangential stresses, would be equal to zero:

$$U_0 = \frac{a^2}{4r^2} (a - x) - \frac{a^3 - x^3}{6r^2} = \left(\frac{r}{r_{k_0}} - 1\right)(a - x) - \frac{a^3 - x^3}{6r^2} \quad (11)$$

Subtracting the value U_0 from the total tangential displacement, we obtain a component caused only by the action of moment M_t :

$$U_t = U - U_0 = \left(\frac{r}{r_k} - \frac{r}{r_{k_0}}\right)(a - x) = \frac{r}{r_{k_0}} \left(\frac{r_{k_0}}{r_k} - 1\right)(a - x) = \frac{r}{r_{k_0}} \xi(a - x), \quad (12)$$

where

$$\xi = \frac{r_{k_0}}{r_k} - 1 \quad (13)$$

As a result, the tangential stresses in the adhesion area, due to the implementation of the thrust force in the contact, will be represented by the dependencies:

$$q_{t_k} = \lambda_{np} U_t = \lambda_{np} \frac{r}{r_{k_0}} \xi(a-x) \quad (14)$$

$$q_{t_{GR}} = -\lambda_{np} U_t = -\lambda_{np} \frac{r}{r_{k_0}} \xi(a-x) \quad (14,a)$$

The corresponding torque on the wheel is found as:

$$M_t = \int_0^a 2bq_{t_k} r dx \quad (15)$$

After substituting dependence (14) and subsequent integration, we obtain:

$$M_t = \lambda_{np} ba^2 r^2 \xi / r_{k_0} = F_t r, \quad (16)$$

where

$$F_t = \int_0^a 2bq_{t_k} dx = \lambda_{np} ba^2 r \xi / r_{k_0} \quad (17)$$

we call the circumferential traction force.

Elementary tangents $dF_t = q_t dx 2b$, distributed along the arc of contact have a resulting F_t located outside the arc of contact.

Let's find the magnitude and line of action of this force.

Each pair of elementary tangential forces “ τ' ” and “ τ'' ” (Fig. 2) acting at points whose coordinates (abscissas) are symmetrical with respect to the midpoint with the coordinate $\alpha_{av} = (\pi/2 + \alpha_0)/2$ has its own resulting:

$$\tau = \sqrt{(\tau')^2 + (\tau'')^2 + 2\tau'\tau'' \cos \varphi}, \quad (18)$$

Passing through the point of intersection of the lines of action τ' and τ'' , located at an angle φ relative to each other.

For points located along the edges, i.e., when $\alpha \rightarrow \alpha_0$ and $\alpha \rightarrow \pi/2$ angle $\varphi \rightarrow \frac{\pi}{2} - \alpha$;

for midpoints, i.e., when $\alpha \rightarrow \alpha_{av}$, the angle is $\varphi \rightarrow 0$.

Let us transform expression (18), presenting it in the following form:

$$\tau = (\tau' + \tau'') \cdot \sqrt{1 + \frac{2\tau'\tau''}{(\tau' + \tau'')^2} (\cos \varphi - 1)} = (\tau' + \tau'') \cdot \sqrt{1 - \frac{\tau'}{\tau''} \frac{\varphi^2}{(1 + \frac{\tau'}{\tau''})^2}} \quad (19)$$

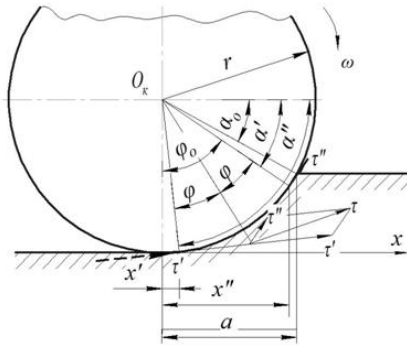


Fig. 2. Elementary tangential forces τ' and τ'' . tangential forces.

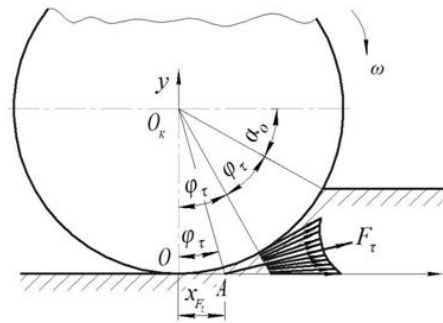


Fig. 3. Diagram of the resulting. elemental

For the extreme and close to them points of the considered contact area $\tau'' \gg \tau'$, therefore, even with a significant wheel immersion depth (for example, when $\varphi \approx 1$), the value of the square root in the last expression (19) differs little from 1. For points located in the middle part of the contact, as before, $\tau'' > \tau'$ (except for the point with $\alpha = \alpha_{av}$, for which $\tau'' = \tau'$ and, in addition (which is more significant), $\varphi \rightarrow 0$ ($\varphi = 0$ at $\alpha = \alpha_{av}$)). Therefore, for the middle contact area the value of the square root is close to 1. This allows us to take in the first approximation $\tau = \tau' + \tau''$.

Taking into account that $\alpha = \arccos \frac{x}{r} \approx \frac{\pi}{2} - \frac{x}{r}$, from where $x = (\frac{\pi}{2} - \alpha)r$ and

$a = (\frac{\pi}{2} - \alpha_0)r$, dependence (14) can be represented as:

$$q_t = \lambda_{np} \xi(\alpha - \alpha_0) r^2 / r_{k_0}$$

Then the values of the elementary tangential forces acting on the symmetrically located elementary areas (Fig. 2) can be found as:

$$\tau' = q'_t 2br d\alpha = \lambda_{np} 2br^3 \xi(\alpha' - \alpha_0) d\alpha / r_{k_0} \quad (20,a)$$

$$\tau'' = q''_t 2br d\alpha = \lambda_{np} 2br^3 \xi(\alpha'' - \alpha_0) d\alpha / r_{k_0} \quad (21,a)$$

For the considered symmetrically located sites

$$\alpha' = \alpha \alpha'' = \pi/2 - (\alpha - \alpha_0) = \pi/2 - \alpha + \alpha_0,$$

what gives

$$\tau' = \lambda_{np} 2br^3 \xi(\alpha - \alpha_0) d\alpha / r_{k_0} \quad (20)$$

$$\tau'' = \lambda_{np} 2br^3 \xi\left(\frac{\pi}{2} - \alpha\right) d\alpha / r_{k_0} \quad (21)$$

As a result:

$$\tau = \tau' + \tau'' = \lambda_{np} 2br^3 \xi\left(\frac{\pi}{2} - \alpha_0\right) d\alpha / r_{k_0} \quad (22)$$

The diagram of the resulting elementary tangential forces is shown in Fig.3.

Summing up these resultants, one can find the magnitude and direction of the total tangential force.

Since the diagram is a system of forces converging at point A (Fig. 3), the total tangential force also passes through this point, being perpendicular to the O_kA line, i.e., at an angle ψ_t to the horizontal. However, from geometrical considerations

$$\psi_t = \psi_\tau / 2 = (\pi/2 - \alpha_0) / 4 \quad (23)$$

Arm $r_\tau = O_kA$ of the action of force F_τ and coordinate x_{F_τ} , which determines the point of application of this force, can be found (Fig. 3) as:

$$r_\tau = O_kA = r / \cos \psi_t \approx r(1 + \psi_t^2 / 2) \approx r \quad (24)$$

$$x_{F_\tau} = r \operatorname{tg} \psi_t \approx r(\pi / 2 - \alpha_0) / 4 \approx r \psi_t \quad (25)$$

When determining the magnitude of the total tangential force, summing up the resulting elementary tangential forces, one should take into account the angles between these resulting ones. However, due to the small size of these angles (which are in the range from 0^0 to $2\psi_t$), their cosines are close to 1 (for example, if we take the average value of the specified angle equal to ψ_t , then at the angle $\alpha_0 = \pi/6$ corresponding to immersion of the wheel into the ground to a depth of $0.5r$, the cosine of the angle ψ_t will be ≈ 0.97). This allows calculating the tangential force using the following formula:

$$F_\tau = \int_{\alpha_0}^{(\pi/2 + \alpha_0)/2} \tau \, da = \int_{\alpha_0}^{(\pi/2 + \alpha_0)/2} \lambda_{np} 2b \xi(\pi/2 - \alpha_0) r^2 d\alpha / r_{k_0} = \lambda_{np} \xi b a^2 r / r_{k_0} \quad (26)$$

Neglecting the indicated angles gives a somewhat overestimated value of the tangential force calculated by the last formula, but this overestimation does not exceed a few percent.

Thus, the actual value of the total tangential force F_t is slightly less than the circumferential traction force F_t calculated by formula (17), and its action arm (see formula (24)) is slightly larger than the radius r . However, these differences are small, and in the future calculations we will assume $F_t = F_t$ and $r_t = r$.

Having a dependence for calculating the tangential force, one can obtain a dependence for finding the rolling radius.

From the equilibrium condition of the driving wheel, it follows that

$$F_{t_x} = F_t \cos \psi_t = F_x + F_{GP} \quad (27)$$

Substituting formula (17), which expresses the force F_t , into this equality, and also taking into account that $\xi = (r_{k_0} / r_k - 1)r / r_{k_0}$, after transformations we will have:

$$r_k = r_{k_0} \frac{r_{k_0}^2}{\lambda_{*p} b a^2 r} F_t = r_{k_0} - \frac{r_{k_0}^2}{\lambda_{*p} b a^2 r \cos \psi_t} (F_{\partial m} + F_x) \quad (28)$$

or

$$r_k = r_k^c - \frac{r_{k_0}^2}{\lambda_{np} b a^2 r \cos \psi_t} F_x, \quad (29)$$

where

$$r_k^c = r_{k_0} - \frac{r_{k_0}^2}{\lambda_{np} b a^2 r \cos \psi_t} F_{GP} \quad (30)$$

- free rolling radius when there is no longitudinal force on the wheel axle.

The presented formulas have the same notation with the formula obtained by E.A. Chudakov. For this reason, the expression represents the coefficient of tangential elasticity of the pair "wheel - deformable ground".

$$\frac{r_{k_0}^2}{\lambda_{np} b a^2 r \cos \psi_t} = \gamma_F \quad (31)$$

Formulas (29) and (28) are also valid for the cases of wheel rolling in braking or driven mode, if the forces F_x and F_t are substituted into the indicated formulas with a minus sign.

The implementation of a tangential force in the contact leads to a change in the normal pressures in the contact by $q_t \cos \alpha = q_x / r$. With the driving wheel, for which $\xi > 0$, the value of normal pressures increases, for the brake wheel it decreases (because $\xi < 0$):

$$q_n = C(H - h)^m + q_t x / r = C(H - h)^m + \lambda_{np} \xi (a - x) x / r$$

In the slip section, taking into account the above, the dependence for the distribution of normal pressures will have the following form:

$$q_n = C(H - h)^m \pm \mu C(H - h)^m x / r = C(H - h)^m (1 \pm \mu x / r)$$

The coordinate of the boundary of the adhesion and sliding sections can be found from the equality $q_t = \mu q_n / \sin \alpha$.

An increase in normal pressures in the contact of the driving wheel and a decrease in them in the contact of the brake wheel leads to the fact that for the same value of the relative loss of speed at $x_B > 0$, a greater tangential force is realized in the contact of the driving wheel than when the brake wheel is rolling. Accordingly, there will be more friction losses in the contact of the driving wheel, and therefore the high power consumption required to roll the wheel on the ground. This is confirmed, in particular, by the experiments of Pirkovsky Yu.V.

The dependences obtained above are valid for the case when the shear stress in the soil is less than the shear stress value at which the upper soil surfaces are sheared.

If the shear of the soil occurs before the tangential stresses reach the cohesion limit, then the picture of the phenomena occurring in the contact and their mathematical description change. When shearing the soil, it must move into the zone of increasing normal pressures. At the same time, with an increase in normal pressures, the allowable stress increases. Due to the movement of the soil layers, there will be friction between them, but there will be no friction losses between the wheels and the ground. The value of the realized tangential force, with the same value of the relative loss of speed, will be even less than in the previous case.

Denoting by $\tau_0 = C + q_n \operatorname{tg} \rho$ (where ρ is the angle of friction between soil particles) the shear stress at which the shear of the soil layers begins, we find the coordinate of the beginning of the shear from the equation:

$$q_t = \lambda_{np} \xi (a - x_B) r / r_{k_0} = \tau_0 \quad (32)$$

$$x_B = a - \frac{\tau_0 r_{k_0}}{\lambda_{np} \xi r} \quad (33)$$

The realized tangential force can be found from the equation:

$$F_t = b \left[\tau_0 (a - x_B)^2 + 2 \int_0^{x_B} \tau dx \right] \quad (34)$$

at $q_t < \tau$ $x_B = 0$

and

$$F_t = \lambda_{np} b a^2 \xi r / r_{k_0} \quad (35)$$

3 Conclusion

In this paper, using the method of motion reversal, the picture of physical phenomena in the contact of the wheel with the ground is considered, which made it possible to obtain relatively simple expressions for calculating the circumferential traction force in the contact of the wheel with the ground (affecting both the performance and the safety of movement of wheeled vehicles on the ground from the point of view of slipping, loss of control, ‘digging’ into the ground) and the coefficient of tangential elasticity of the pair “wheel - deformable ground”.

References

1. T.A. Balabina, Y.I. Brovkina, A.N. Mamaev, Lecture Notes in Mechanical Engineering **9783319956299**, 2027-2035 (2019) DOI: 10.1007/978-3-319-95630-5_218
2. T.A. Balabina, M.Yu. Karelina, A.N. Mamaev, AIP conference Proceedings. Ser. "Proceedings International Conference "Problems of Applied Mechanics"" **040004** (2021) DOI: 10.1063/5.0047307
3. T.A. Balabina, M.Yu. Karelina, A.N. Mamaev, AIP Conference Proceedings. Ser. "Proceedings International Conference "Problems of Applied Mechanics"" **040002** (2021) DOI: 10.1063/5.0047299
4. E.V. Balakina, *J Fric Wear* **40(6)**, 573–579 (2019) <https://doi.org/10.3103/S1068366619060047>
5. E.V. Balakina, M. Kotchetov, D. Serbaev, *Transportation Research Procedia* **57**, 100-108 (2021)
6. E.V. Balakina, I. Sergienko, *Transportation Research Procedia* **57**, 92-99 (2021)
7. E. Bakker, L. Nyborg, H. Pacejka, Tyre modeling for use in vehicle dynamics studies SAE Technical Paper **870421** (1980)
8. M.G. Becker, Introduction to the theory of the "terrain-machine" system (M., Mechanical Engineering, 1973)
9. J. Cho, S. Lee, H.Y. Jeong, *Finite Elem. Anal. Des.* **105**, 26-32 (2015) DOI:10.1016/J.FINEL.2015.06.009
10. S.K. Clark, *Tire rolling resistance* (ACS, 1983)
11. S. Evtukov, I. Gladushevskiy, El. Kurakina, *Transportation Research Procedia* **57**, 145-153 (2021)
12. A. Emami, et al., *Proc. ASME 2017 10th Annual Dynamic Systems and Control Conf., Am. Soc. Mech. Eng.* **6** (2017)
13. D. Fujiwara, N. Tsujikawa, T. Oshima et al, *Journal of Terramechanics* **94**, 1-12 (2021) <https://doi.org/10.1016/j.jterra.11.004>
14. G. Ginzburg, S. Evtiukov, I. Brylev, S. Volkov, *Transportation Research Procedia* **20**, 212–218 (2017) DOI: 10.1016/j.trpro.2017.01.054
15. G. Gim, *Int J Veh Des* **11**, 589-618 (1990)
16. E. Jimenez, C. Sandu *Tire Sci Technol* **48(1)**, 22–45 (2020)
17. M.Y. Karelina, T.A. Balabina, A.N. Mamaev, *Proceedings of the 5th International Conference on Industrial Engineering (ICIE 2019). Lecture Notes in Mechanical Engineering*, 531-540 (2019) DOI: 10.1007/978-3-030-22063-1_56

18. M.Yu. Karelina, T.A. Balabina, T.Yu. Cherepnina, A.N. Mamaev, A.S. Vorontsov, IOP Conference Series: Materials Science and Engineering **832**, 012078 (2020)
DOI: 10.1088/1757-899X/832/1/012078
19. M.Yu. Karelina, T.A. Balabina, V.V. Filatov, A.N. Mamaev, A.S. Vorontsov, IOP Conference Series: Materials Science and Engineering **832**, 012079 (2020)
DOI: 10.1088/1757-899X/832/1/012079
20. J. Kurjenluoma, L. Alakukku, J. Ahokas, Journal of Terramechanics **46(6)**, 267-275 (2009) <https://doi.org/10.1016/j.jterra.2009.07.002>
21. H.D. Kutzbach, A. Bürger, S. Böttinger, Journal of Terramechanics **82**, 13-21 (2019)
<https://doi.org/10.1016/j.jterra.2018.11.002>
22. S. Khaleghian, O. Ghasemalizadeh, S. Taheri, Tire Sci. Technol. **44(4)**, 248–261 (2016)
23. A.I. Kubba, G.J. Hall, S. Varghese, O.A. Olatunbosun, C.J. Anthony, Tire Sci. Technol. **46(2)**, 78–92 (2018)
24. J. Li, Y. Zhang, J. Yi, J. DynSystMeas Control Trans. ASME **135**, 359-370 (2012)
DOI:10.1115/1.4006887
25. W. Liang, J. Medanic, R. Ruhl, Veh. Syst. Dyn. **46**, 197–227 (2008)
26. L. Damme, P. Schjonning, L.J. Munkholm et al., Soil and Tillage Research **211**, 105.020 (2021)
27. R.M. Makharoblidze, M. Lagvilava, B.B. Basilashvili, Annals of Agrarian Science **16(1)**, 65-68 (2017) <https://doi.org/10.1016/j.aasci.12.010>
28. A. Mamaev, T. Balabina, M. Karelina, Transportation Research Procedia. 14. Ser. "14th International Conference on Organization and Traffic Safety Management in Large Cities, OTS 2020", 430-435 (2020) DOI: 10.1016/j.trpro.2020.10.051
29. A.N. Mamaev, T.A. Balabina, I.V. Odinkova, V.V. Gaevskiy, IOP Conference Series: Materials Science and Engineering **632**, 012083 (2019) DOI: 10.1088/1757-899X/632/1/012083
30. M. Viehweger et al., Vehicle System Dynamics, 1–28 (2020)
<https://doi.org/10.1080/00423114.2020.1714672>
31. S. Ozaki, W. Kondo, J. Terramech **64**, 1-9 (2016) DOI:10.1016/j.jterra.2015.12.001
32. S. Papamichael, C. Vrettos, Journal of Terramechanics **94**, 39-48 (2021)
33. H.B. Pacejka, Tire and Vehicle Dynamics (Amsterdam, Elsevier, 2012)
34. V. Pryadkin, A. Artemov, P. Kolyadin, Transportation Research Procedia **57**, 502-510 (2021)
35. M. Viehweger et al., Veh. Syst. Dyn. **1**, 1–28 (2020)
36. J. Wong, Theory of land vehicles (M., Mechanical Engineering, 1982)
37. V.N. Zadvornov et al., J Frict Wear **41(4)**, 354–358 (2020)
<https://doi.org/10.3103/S1068366620040145>